

Supramolecular motifs in metal complexes of Schiff bases.

Part 6.¹ Topology of two types of self-assembly of bis-*N,O*-bidentate Schiff base ligands by copper(II) ions †

2 PERKIN

Noboru Yoshida,^{*a} Hiroki Oshio^b and Tasuku Ito^b

^a Laboratory of Molecular Functional Chemistry, Division of Material Science, Graduate School of Environmental Earth Science, Hokkaido University, Sapporo, 060-0810, Japan

^b Department of Chemistry, Graduate School of Science, Tohoku University, Sendai, 980-8578, Japan

Received (in Cambridge, UK) 1st May 2001, Accepted 19th June 2001

First published as an Advance Article on the web 31st July 2001

Two examples of copper(II)-assisted self-assembly of bis-*N,O*-bidentate Schiff base ligands **L**⁵⁵ and **L**⁵⁶ with an aromatic spacer group are described. Single-crystal X-ray analyses demonstrated clearly the formation of a tetranuclear double-helical architecture for the **L**⁵⁵-Cu^{II} system and a dinuclear non-helical U-shaped one for the **L**⁵⁶-Cu^{II} system. The self-assembly process for these systems in solution has been deduced from UV-vis and ESI mass spectral and analytical data. Aromatic $\pi \cdots \pi$ and CH $\cdots\pi$ interactions between the spacer groups in **L**⁵⁵ and **L**⁵⁶ could stabilize these unprecedented supramolecular motifs in solution and the solid state. Their crystal packings are also controlled by the aromatic interactions between two entities.

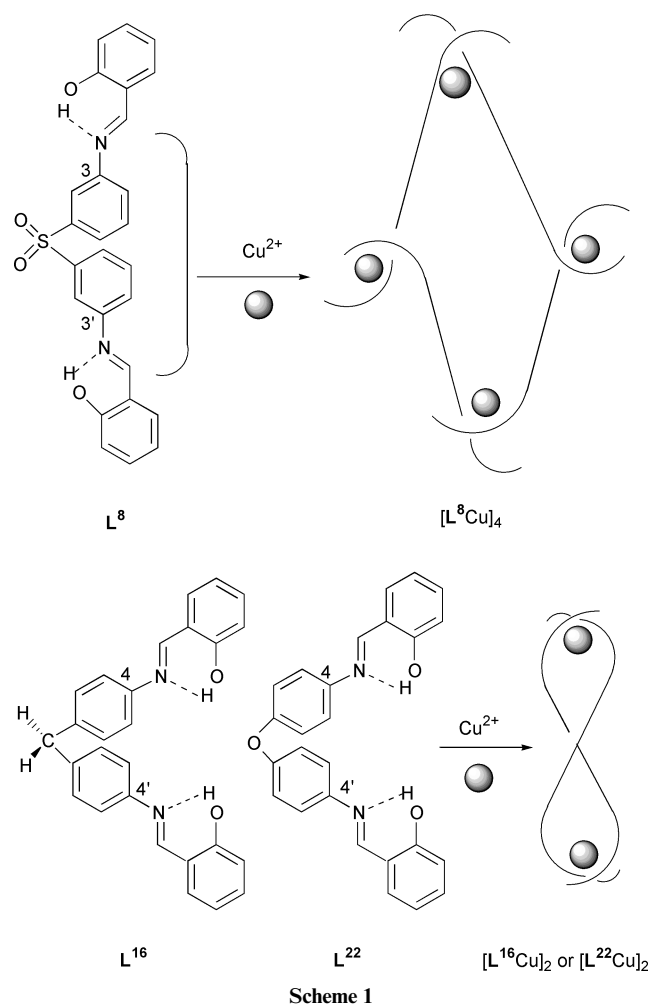
Introduction

Research on supramolecular motifs formed by the self-assembly of their constituent components as building blocks using noncovalent interactions is structurally of great importance as a basis for future nanomachine technologies.²

We have reported a simple synthetic method for the metal-assisted self-assembly of complexes using commercially available starting materials to extend the wide range of well-defined supramolecular architecture.^{1,3-6} Our recent X-ray crystallographic studies performed on a variety of Cu(II) complexes of Schiff base ligands, **L**⁸, **L**¹⁶ and **L**²² (Scheme 1), revealed that the final fine-tuning of supramolecular architectures such as the dinuclear double-helical and/or tetranuclear double-helical structure is greatly controlled by the π - π and CH- π interactions between the spacer groups which could bridge two metal-coordination sites.⁶ Furthermore, the steric positional requirement such as a 3,3' linkage (**L**⁸) and a 4,4' linkage (**L**¹⁶ and **L**²²) of the spacer group in the ligand, which could induce an effective π - π interaction, may be related to the cluster interconversion from the tetranuclear structure to the dinuclear one. Cluster interconversion phenomena have been observed in some helical complexes upon changing the ligand structure and including a guest molecule.⁷

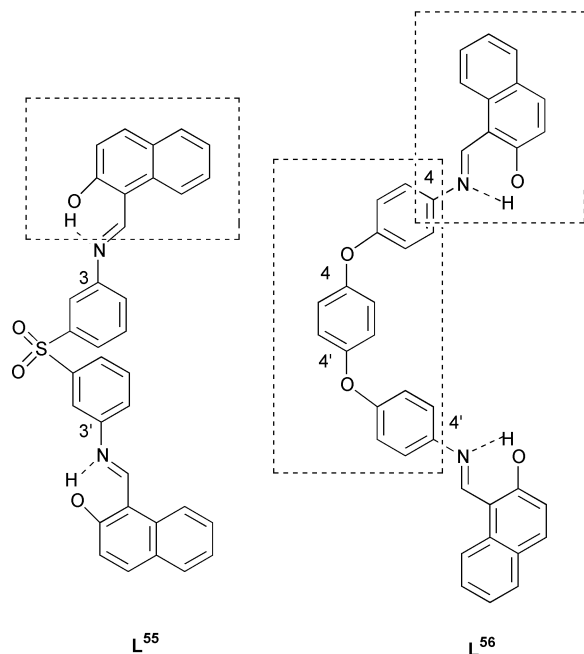
In this paper, we describe the synthesis and characterization of the supramolecular architectures formed by the Cu^{II}-assisted self-assembly of the bis-*N,O*-bidentate Schiff base ligands **L**⁵⁵ and **L**⁵⁶ with an aromatic spacer group as shown in Scheme 2.

The ligand **L**⁵⁵ possesses a 3,3'-linkage position in the spacer group (Scheme 2) which would be closely related to the formation of the tetranuclear double-helical motif observed in the **L**⁸-Cu^{II} system in Scheme 1. Furthermore, we expect that the naphthalene coordination site in the ligand **L**⁵⁵ may lead to



† Electronic supplementary information (ESI) available: figures showing space-filling representation of **1** (Fig. S1), molecular square cavity in the central bridging moiety (Fig. S2), channel structures of **2** along the *a* axis (Fig. S3) and packing of the U-shaped bridging non-helical structures of **2** (Fig. S4). See <http://www.rsc.org/suppdata/p2/b1/b103902b/>

effective overlap between the aromatic-aromatic interactions. On the other hand, the ligand **L**⁵⁶ has a naphthalene moiety and a 4,4'-linkage position in the longer spacer group (-C₆H₄-O-



Scheme 2

$C_6H_4-O-C_6H_4-$) as compared with that ($-C_6H_4-O-C_6H_4-$) of the ligand **L**²². The unprecedented resulting entities may be induced by such a subtle change in the ligand structure. Copper(II) ions which are a key functional factor in many copper-containing enzymes were selected as a primary ligand assembling unit because their non-preferential coordination geometry has been frequently observed.

Experimental

Syntheses of **L**⁵⁵ and **L**⁵⁶ and their copper(II) complexes

L⁵⁵ was prepared in 93% yield by mixing ethanolic solutions of bis(3-aminophenyl) sulfone (0.02 mol) and 2-hydroxy-1-naphthaldehyde (0.04 mol). The brilliant-yellow solution obtained was stirred for 30 min at 60–70 °C. The orange-colored solid that formed was collected by filtration and air-dried. Found: C, 73.08; H, 4.50; N, 5.26%; $C_{34}H_{24}N_2O_4S$ requires C, 73.36; H, 4.34; N, 5.03%. **L**⁵⁶ was also obtained as an orange solid from the Schiff-base condensation in ethanol of 1,4-bis(4-aminophenoxy)benzene (0.025 mol) and 2-hydroxy-1-naphthaldehyde (0.05 mol). Found: C, 80.10; H, 4.81; N, 4.62%; $C_{40}H_{28}N_2O_4$ requires C, 79.98; H, 4.69; N, 4.66%.

Copper(II) complexes, **1** and **2**, were prepared by the reactions between **L**⁵⁵ and **L**⁵⁶ and copper(II) acetate monohydrate in hot ethanolic solutions and DMF solutions at room temperature, respectively, according to previously reported procedures.⁶ Found: C, 65.35; H, 3.73; N, 4.66%; $C_{136}H_{88}Cu_4N_8O_{16}S_4$ as $Cu_4(L^{55} - 2H)_4$ requires C, 66.08; H, 3.58; N, 4.53%; Found: C, 70.56; H, 4.40; N, 5.28%; $C_{84.5}H_{62.5}Cu_2N_{5.5}O_{9.5}$ as $Cu_2(L^{56} - 2H)_2 \cdot 1.5DMF$ requires C, 70.77; H, 4.39; N, 5.37%.

X-Ray crystal structure determinations

Single crystals of **1** and **2** suitable for X-ray crystallography were obtained by slow diffusion of diethyl ether into a chloroform solution of the complexes at room temperature. Crystal data for complexes **1** and **2** are reported in Table 1. Suitable crystals were quickly transferred from the mother liquor to a stream of cold N_2 on a Rigaku AFC 7S with a CCD-type area detector. All diffraction data were collected at low temperature using graphite-monochromated Mo-K α radiation. The structure was solved by direct methods with SHELXS-97^{8a} and Fourier techniques and refined by full-matrix least-squares on F2 data using SHELXL-97.^{8b}

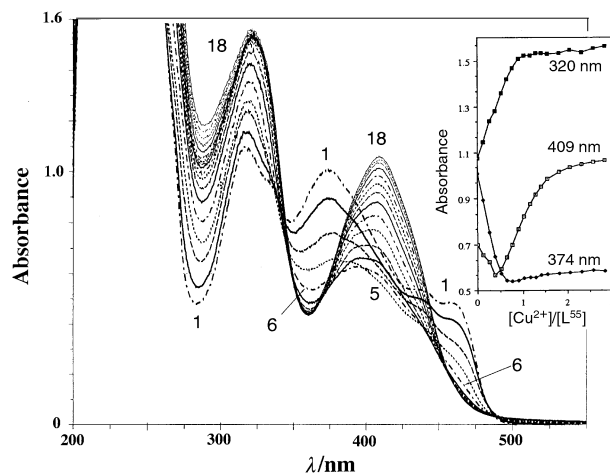


Fig. 1 UV-vis spectral change of ligand **L**⁵⁵ in ethanol upon addition of $Cu(CH_3COO)_2 \cdot H_2O$. $[L^{55}] = 6.50 \times 10^{-5} \text{ mol dm}^{-3}$. $[Cu^{II}] = 0, 0.83, 1.66, 2.49, 3.32, 4.15, 4.98, 5.81, 6.64, 7.47, 8.30, 9.13, 9.96, 10.29, 11.62, 12.45, 13.28 \times 10^{-5} \text{ mol dm}^{-3}$.

CCDC reference numbers 163701 and 163702. See <http://www.rsc.org/suppdata/p2/b1/b103902b/> for crystallographic data in CIF or other electronic format.

Molecular graphics calculations were performed with ORTEP-3.⁹

Results and discussion

UV-vis titration of **L**⁵⁵ with Cu^{II} ion

Fig. 1 shows the change in the UV-vis spectrum which occurs when **L**⁵⁵ coordinates to Cu^{II} ions in EtOH. A very complicated spectral pattern characteristic of the enol (409 nm) and keto (438 and 463 nm) forms in the ligand **L**⁵⁵ is observed. Upon addition of Cu^{II} ions to the ligand solution, the ligand $\pi-\pi^*$ bands at 374, 438 and 463 nm decrease and the shorter band at 320 nm increases. The isosbestic point at 338 nm is gradually red-shifted several nm and a new broad band at 409 nm due to the deprotonation of the OH group and the *N,O*-coordination to Cu^{II} ion⁶ emerges when $[Cu^{II}]/[L^{55}] = 0.4-0.5$. A mole ratio plot using the changes in absorbance at 320 nm clearly demonstrates the formation of a $Cu^{II} : L^{55} = 1 : 1$ complex. However, further addition of Cu^{II} ion led to an additional increase in absorbance at 400 nm and a saturation at $[Cu^{II}]/[L^{55}] = ca. 2$. This suggests a structural switching at the higher Cu^{II} concentration.⁶

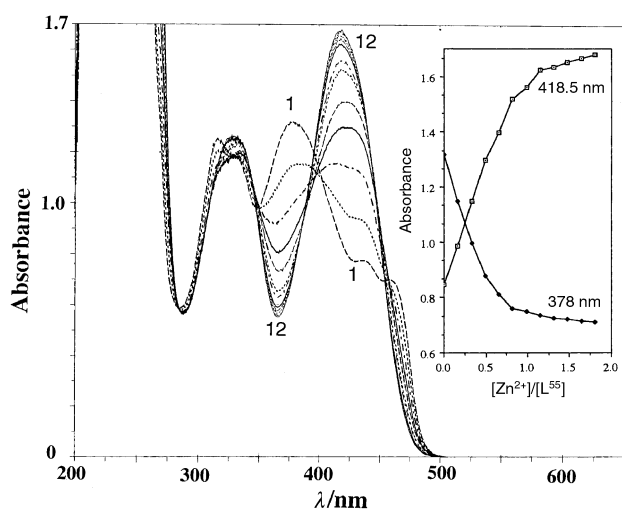
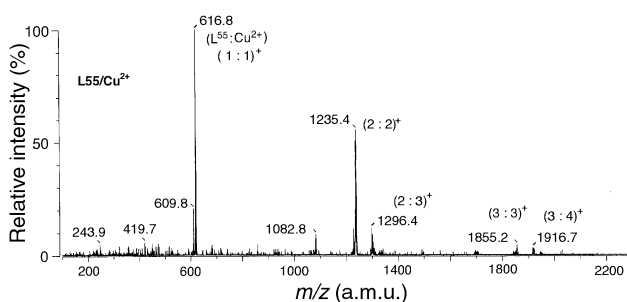
More simple UV-vis spectral changes with both a decrease in the ligand band at 378 nm and an increase in a new band at 418.5 nm are observed in the $Zn^{II}-L^{55}$ system as shown in Fig. 2. Their saturations take place at a value of exactly $[Zn^{II}]/[L^{55}] = 1$ (the inset in Fig. 2), indicating the formation of a $Zn^{II} : L^{55} = 1 : 1$ complex. A particular preference for square planar, tetrahedral and/or octahedral coordination geometry of Cu^{II} and Zn^{II} ions may have an appreciable influence on the self-assembly of **L**⁵⁵ in solution.

ESI MS spectrum of the **L**⁵⁵- Cu^{II} complex **1**

Positive electrospray ionization mass spectroscopy (ESI-MS) of the **L**⁵⁵- Cu^{II} complex, **1** in MeOH (trace $CHCl_3$) shows the presence of several aggregated species (Fig. 3). Some weak peaks at $m/z = 1296.4, 1855.2$ and 1916.7 could be assigned to trinuclear species, $(L^{55} : Cu^{II} = 2 : 3)^+$ and $(3 : 3)^+$, and tetranuclear species such as $(3 : 4)^+$. Two stronger peaks at $m/z = 616.8$ and 1235.4 would correspond to mononuclear $(1 : 1)^+$ and binuclear $(2 : 2)^+$ species. Thus, the well resolved positive ESI spectrometric analysis provided no proof of the existence of tetranuclear species $(4 : 4)^+$ in MeOH solution due to the poor solubility of complex **1**.

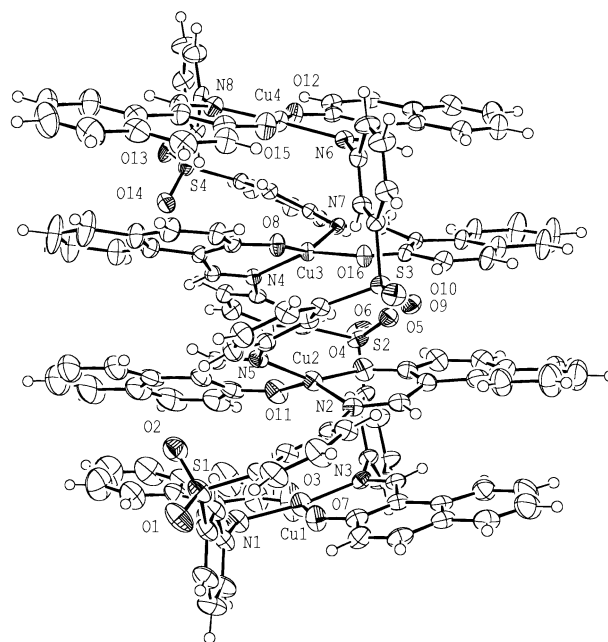
Table 1 Crystallographic data for $[\text{Cu}^{\text{II}}(\text{L}^{55} - 2\text{H})]_4 \cdot \text{CHCl}_3 \cdot 2\text{Et}_2\text{O}$, $1 \cdot \text{CHCl}_3 \cdot 2\text{Et}_2\text{O}$ and $[\text{Cu}^{\text{II}}(\text{L}^{56} - 2\text{H})]_2 \cdot 2\text{CHCl}_3 \cdot \text{Et}_2\text{O}$, $2 \cdot 2\text{CHCl}_3 \cdot \text{Et}_2\text{O}$

	1·CHCl ₃ ·2Et ₂ O	2·2CHCl ₃ ·Et ₂ O
Formula	C ₁₄₅ H ₁₀₉ Cl ₃ Cu ₄ N ₈ O ₁₈ S ₄	C ₈₆ H ₆₄ Cl ₆ Cu ₂ N ₄ O ₉
<i>M</i>	2740.310	1637.284
Crystal system	Triclinic	Monoclinic
Space group	<i>P</i> $\bar{1}$	<i>P</i> 2 ₁ / <i>c</i>
Unit dimensions		
<i>a</i> /Å	16.3594(8)	12.6528(10)
<i>b</i> /Å	18.2027(9)	20.1218(15)
<i>c</i> /Å	24.3250(13)	30.263(3)
<i>a</i> ^o	84.810(1)	
<i>β</i> ^o	86.790(1)	100.815(10)
<i>γ</i> ^o	65.321(6)	
<i>V</i> /Å ³	6553.7(6)	7567.9(10)
<i>Z</i>	2	4
<i>T</i> /K	173	173
<i>D</i> /g cm ⁻³	1.388	1.430
<i>μ</i> /mm ⁻¹	0.831	0.837
<i>λ</i> (Mo-Kα)/Å	0.71073	0.71073
Reflections collected	28611	52032
Independent reflections	28611 [<i>R</i> (int) = 0.000]	14946 [<i>R</i> (int) = 0.0574]
Final <i>R</i> ₁ , <i>wR</i> ₂ [<i>I</i> > 2σ(<i>I</i>)]	0.0603, 0.1577	0.0520, 0.1410
<i>R</i> indices (all data)	0.1218, 0.1936	0.0749, 0.1560

**Fig. 2** UV-vis spectral change of ligand L^{55} in ethanol upon addition of $\text{Zn}(\text{CH}_3\text{COO})_2 \cdot 2\text{H}_2\text{O}$. $[\text{L}^{55}] = 7.19 \times 10^{-5} \text{ mol dm}^{-3}$. $[\text{Zn}^{\text{II}}] = 0, 1.06, 2.12, 3.18, 4.24, 5.30, 6.36, 7.42, 8.48, 9.54, 10.6, 11.66 \times 10^{-5} \text{ mol dm}^{-3}$.**Fig. 3** ESI mass spectrum of a methanol solution of **1**.

X-Ray crystal structure of the $\text{L}^{55}\text{-Cu}^{\text{II}}$ complex, **1**

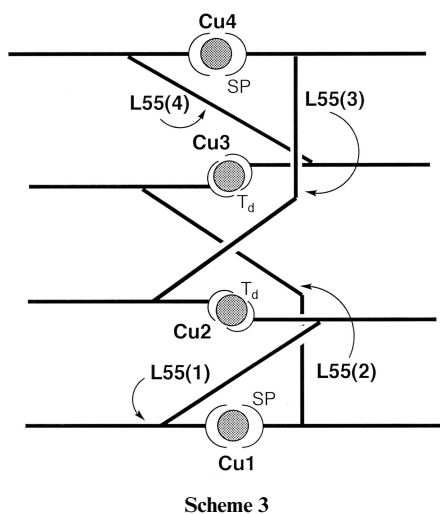
Fig. 4 shows the molecular structure of tetranuclear double-helical $[\text{Cu}^{\text{II}}(\text{L}^{55} - 2\text{H})]_4$ complex **1**. The isolation of a 4 : 4 complex in the solid state does not mean that this is the most stable species in solution as mentioned in the ESI-MS study. The neutral complex **1** contains four Cu^{II} ions with two different coordination geometries and four L^{55} ligands with two types of conformations (*vide infra*). Selected bond lengths and angles are presented in Table 2. The average Cu–N(azomethine N) and Cu–O distances are 1.97 Å and 1.90 Å, respectively.

**Fig. 4** An ORTEP representation of the structure of neutral complex **1**, $[\text{Cu}^{\text{II}}(\text{L}^{55} - 2\text{H})]_4$ nearly perpendicular to the Cu1–Cu4 vector (50% probability thermal ellipsoids).

The CPK representation shown in the electronic supplementary data † (Fig. S1) indicates clearly the function of multiple π – π aromatic interactions in the Cu^{II} -assisted spontaneous assembly of L^{55} into double-helical architecture. This well-defined stacking structure with π – π interactions at 3.2–3.9 Å would be due to the prolonged naphthalene moiety in L^{55} . Scheme 3 shows a schematic representation of the neutral complex **1**. The coordination geometry around the outer Cu^{II} ions such as Cu1 and Cu4 appears to be a strictly square-planar (SP) coordination geometry but the inner Cu^{II} ions (Cu2 and Cu3) display a distorted tetrahedral (T_d) coordination geometry. Furthermore, two types of conformers of ligand L^{55} are clearly observed in structure **1**. Two ligands $\text{L}^{55}(1)$ and $\text{L}^{55}(4)$ show the *anti*-closed form as shown in Scheme 4. The other *anti*-opened conformer in ligands $\text{L}^{55}(2)$ and $\text{L}^{55}(3)$ differs significantly from that in $\text{L}^{55}(1)$ and $\text{L}^{55}(4)$. The four Cu^{II} ions in **1** with SP and T_d coordination geometry are almost in plane and reveal almost the same rhombic arrangement as found in the $[\text{Cu}^{\text{II}}(\text{L}^8 - 2\text{H})]_4$ complex (Fig. 5).⁶ Therefore,

Table 2 Selected bond lengths (Å) and angles (°) for $[\text{Cu}^{\text{II}}(\text{L}^{55} - 2\text{H})_4]$ **1** with esds in parentheses

Cu–N and Cu–O			
Cu(1)–O(3)	1.884(4)	Cu(1)–O(7)	1.895(4)
Cu(1)–N(3)	1.951(4)	Cu(1)–N(1)	1.965(4)
Cu(2)–O(4)	1.894(3)	Cu(2)–O(11)	1.900(3)
Cu(2)–N(5)	1.959(4)	Cu(2)–N(2)	1.978(4)
Cu(3)–O(8)	1.900(3)	Cu(3)–O(16)	1.907(3)
Cu(3)–N(4)	1.964(3)	Cu(3)–N(7)	1.977(3)
Cu(4)–O(15)	1.886(3)	Cu(4)–O(12)	1.908(3)
Cu(4)–N(6)	1.960(4)	Cu(4)–N(8)	1.966(4)
C=N			
N(1)–C(7)	1.311(6)	N(3)–C(41)	1.300(6)
N(2)–C(24)	1.315(5)	N(5)–C(75)	1.315(6)
N(4)–C(58)	1.317(5)	N(7)–C(109)	1.314(5)
N(6)–C(92)	1.312(5)	N(8)–C(126)	1.307(5)
–SO ₂ –			
S(1)–O(2)	1.446(4)	S(1)–O(1)	1.455(4)
S(2)–O(5)	1.441(3)	S(2)–O(6)	1.454(3)
S(3)–O(9)	1.441(3)	S(3)–O(10)	1.454(3)
S(4)–O(14)	1.437(3)	S(4)–O(13)	1.447(3)
O(3)–Cu(1)–O(7)	169.0(2)	O(3)–Cu(1)–N(3)	88.80(17)
O(7)–Cu(1)–N(3)	91.28(15)	O(3)–Cu(1)–N(1)	89.77(17)
O(7)–Cu(1)–N(1)	91.55(16)	N(3)–Cu(1)–N(1)	172.35(17)
O(4)–Cu(2)–O(11)	89.05(14)	O(4)–Cu(2)–N(5)	150.88(15)
O(11)–Cu(2)–N(5)	92.74(15)	O(4)–Cu(2)–N(2)	93.20(15)
O(11)–Cu(2)–N(2)	147.82(15)	N(5)–Cu(2)–N(2)	100.42(15)
O(8)–Cu(3)–O(16)	86.82(12)	O(8)–Cu(3)–N(4)	92.82(13)
O(16)–Cu(3)–N(4)	153.29(14)	O(8)–Cu(3)–N(7)	151.10(14)
O(16)–Cu(3)–N(7)	93.47(13)	N(4)–Cu(3)–N(7)	99.41(14)
O(15)–Cu(4)–O(12)	177.76(15)	O(15)–Cu(4)–N(6)	88.01(14)
O(12)–Cu(4)–N(6)	91.06(14)	O(15)–Cu(4)–N(8)	90.63(15)
O(12)–Cu(4)–N(8)	90.40(14)	N(6)–Cu(4)–N(8)	177.01(15)



the strictly reproduced Cu^{II} ion array with a tetranuclear cluster in $[\text{Cu}^{\text{II}}(\text{L}^{55} - 2\text{H})_4]$ and $[\text{Cu}^{\text{II}}(\text{L}^8 - 2\text{H})_4]$ requires the 3,3'-linkage position at the spacer group (Scheme 2) against the –SO₂– group in the ligands L⁵⁵ and L⁸.

UV-vis titration of L⁵⁶ with Cu^{II} ion

The UV-vis change in the L⁵⁶–Cu^{II} complexation (Fig. 6) differs significantly from that in the L⁵⁵–Cu^{II} system, which displays a simple continuous variation with four isosbestic points. A mole ratio plot using the change in absorbance at 463.5 nm clearly demonstrated the formation of the Cu^{II} : L⁵⁶ = 1 : 1 complex, as judged by observing the clear inflection point at $[\text{Cu}^{\text{II}}]/[\text{L}^{56}] = 1$.

ESI MS spectrum of the L⁵⁶–Cu^{II} complex, **2**

Fig. 7 shows the positive ESI-MS (in MeOH with trace CHCl₃)

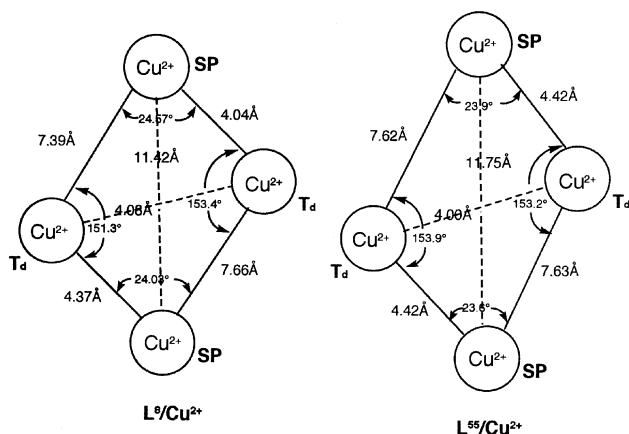


Fig. 5 Two rhombic arrangements of the four Cu(II) ions found in **1** and **2**.

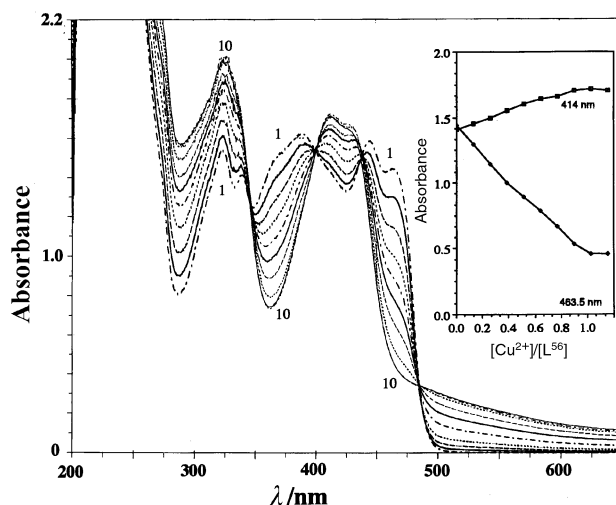
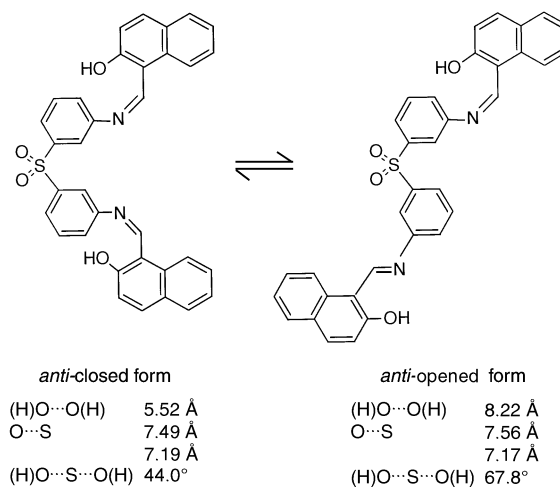


Fig. 6 UV-vis spectral change of ligand L⁵⁶ in ethanol upon addition of Cu(CH₃COO)₂·H₂O. $[\text{L}^{56}] = 6.50 \times 10^{-5} \text{ mol dm}^{-3}$. $[\text{Cu}^{\text{II}}] = 0, 0.83, 1.66, 2.49, 3.32, 4.15, 4.98, 5.81, 6.64, 7.47, 8.30$ (turbid) $\times 10^{-5} \text{ mol dm}^{-3}$.



for **2**. It is noteworthy that in methanol solution a primary dinuclear (2 : 2)⁺ species corresponding to $[\text{L}^{56} - 2\text{H} - \text{Cu}^{\text{II}}]_2$ is observed at $m/z = 1325.0$. The relatively strong peaks at $m/z = 662.0$ and 1988.1 are associated with mononuclear (1 : 1)⁺ and trinuclear (3 : 3)⁺ aggregate species. The trinuclear species and the tetranuclear species are also observed at $m/z = 1355.6$ and 2648.9, respectively.

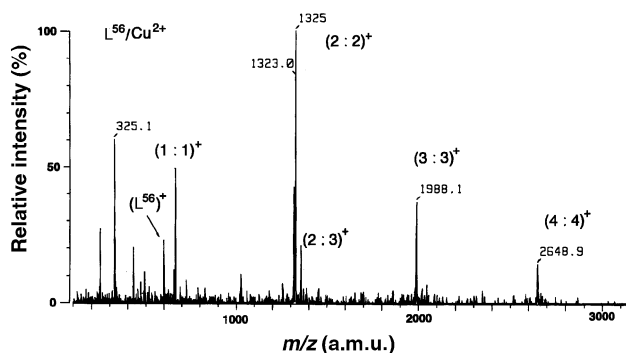


Fig. 7 ESI mass spectrum of a methanol solution of **2**.

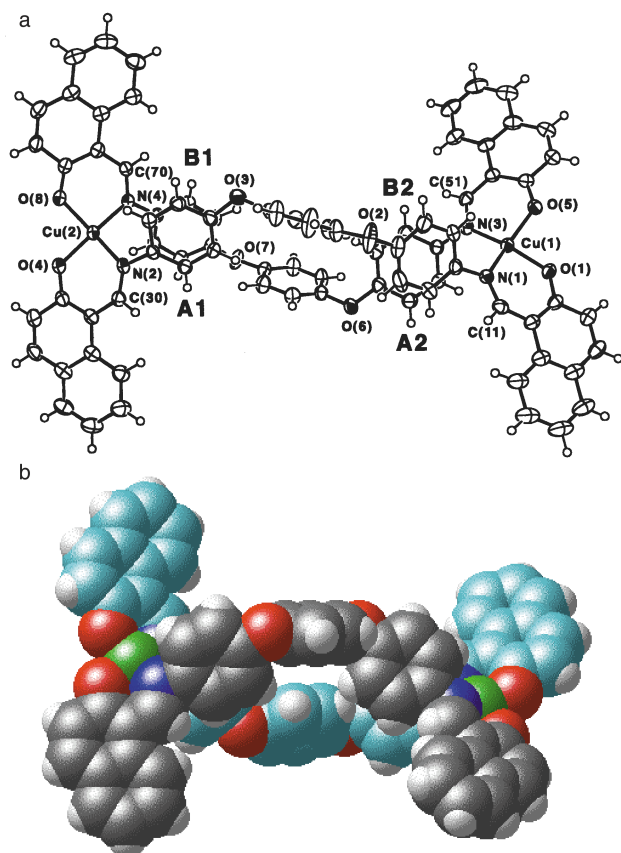
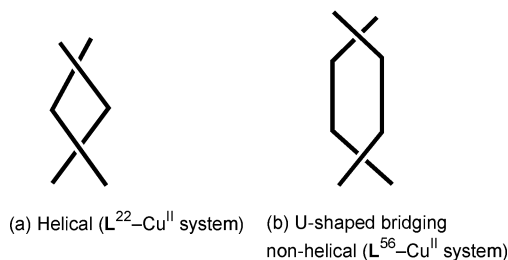


Fig. 8 (a) An ORTEP representation of the structure of neutral complex **2**, $[\text{Cu}^{\text{II}}(\text{L}^{56} - 2\text{H})_2]$. (b) CPK representation of **2**.

X-Ray crystal structure of the $\text{L}^{56}\text{-Cu}^{\text{II}}$ complex, **2**

The single crystal structure in Fig. 8(a) provided the ultimate proof of the proposed dinuclear cluster for **2**; a CPK represen-



Scheme 5

tation is shown in Fig. 8(b). Selected bond lengths and angles are presented in Table 3. The neutral complex **2** is constructed from two Cu^{II} ions and two L^{56} ligands and its structure is not double-helical but is a U-shaped bridging non-helical one (Scheme 5) due to the longer spacer group ($-\text{C}_6\text{H}_4\text{-O-C}_6\text{H}_4\text{-O-C}_6\text{H}_4-$) and the $\pi \cdots \pi$ interactions (3.12–3.78 Å) between $\text{A1} \cdots \text{B1}$ and $\text{A2} \cdots \text{B2}$ benzene rings. The formation of a U-shaped structure could arise partly from the steric hindrance between the plane of phenyl moieties $\text{A1}(\text{B1})$ and $\text{A2}(\text{B2})$ and that of the naphthyl group. A relatively large square cavity (O3-O7-O6-O2 , $6.46 \times 5.51 \text{ \AA}^2$) could be formed in the central bridging moiety (ESI, Fig. S2).[†] This macro cavity extends along the a -axis as shown in Fig. S3,[†] affording a 2D square grid network. The ligand L^{22} with a shorter spacer such as $-\text{C}_6\text{H}_4\text{-O-C}_6\text{H}_4-$ has been found to form a double helical architecture.⁶ A projection of the crystal packing with no solvents of **2** in the a - c plane is presented in Fig. S4.[†] Intermolecular and $\pi \cdots \pi$ and $\text{CH} \cdots \pi$ interactions at various moieties of **2** lead to the mutual-embraced packing form in the a - c plane.

References

- 1 For Part 5, see N. Yoshida, K. Ichikawa and M. Shiro, *J. Chem. Soc., Perkin Trans. 2*, 2000, 17.
- 2 V. Balzani, A. Credi, F. M. Raymo and J. F. Stoddart, *Angew. Chem., Int. Ed.*, 2000, **39**, 3348; J.-M. Lehn, *Supramolecular Chemistry—Concepts and Perspectives*, VCH, Weinheim, 1995.
- 3 N. Yoshida and K. Ichikawa, *Chem. Commun.*, 1997, 1091.
- 4 N. Yoshida, H. Oshio and T. Ito, *Chem. Commun.*, 1998, 63.
- 5 N. Yoshida, N. Ito and K. Ichikawa, *J. Chem. Soc., Perkin Trans. 2*, 1997, 2387.
- 6 N. Yoshida, H. Oshio and T. Ito, *J. Chem. Soc., Perkin Trans. 2*, 1999, 975.
- 7 M. Scherer, D. L. Caulder, D. W. Johnson and K. N. Raymond, *Angew. Chem., Int. Ed.*, 1999, **38**, 1588; C. M. Hartshorn and P. J. Steel, *Chem. Commun.*, 1997, 541; J. S. Fleming, K. L. V. Mann, C.-A. Carraz, E. Psillakis, J. C. Jeffery, J. A. McCleverty and M. D. Ward, *Angew. Chem., Int. Ed.*, 1998, **37**, 1279; P. N. W. Baxter, G. Hanan and J.-M. Lehn, *Chem. Commun.*, 1996, 2019.
- 8 (a) SHELXS-97, G. M. Sheldrick, University of Göttingen, 1990; (b) SHELXL-97, G. M. Sheldrick, University of Göttingen, 1997.
- 9 ORTEP3 for Windows (Version 1.05), L. J. Farrugia, Department of Chemistry, University of Glasgow, 1999.